DAFTAR PUSTAKA

Ahmad, W. (2005). Fundamentals of chemistry, mineralogy, weathering processes, formation, and exploration. Unpublished.

Ahmad, W. (2002). Nickel Laterites-A Short Course : Chemistry, Mineralogy, and Formation of Nickel Laterites. Unpublished

Andrews, L. (2004). Factors affecting nickel recovery from slags produced during platinum smelting. VIIInternational Conferenceon Moltem Slagsfluxesand salts. The South African InstituteofMiningand Metallurgy.

Asy'ari, H., Aris B., Agus M,. (2013). "Speed Bump Sebagai Pembangkit Listrik Ramah Lingkungan Dan Terbarukan". Jurnal Seminar Nasional Teknologi Informasi & Komunikasi Terapan 2013 (Semantik 2013). Semarang.

Brand, N.W. Butt, C.R.M. Elias, M. (199)8. *Nickel Laterite: classification and feature.*
AGSO Journal of Australian Gology & Geophysics, 17 (4), 81- 88.

Bulatovic, S.M. (2007). Handbook of Flotation Reagents volume 1. Amsterdam: Elsevier.p. 443.

Crundwell, F. K., Moats, M. S., Ramachandran, V., Robinson, T. G., and Davenport, W. G. (2011). Hydrometalurgy. Oxford: Elservier.

Cui, H., Anderson, C. G. (2016). Literature Review of Hydrometallurgical Recycling of Printed Circuit Boards (PCBs). J Adv Chem Eng 6: 142. doi:10.4172/2090- 4568.1000142.

Dalvi D.A, W. G. B. and Robert C. Osborne. (2004). The Past and the Future of Nickel Laterites Paper presented at the British Library Conference Proceedings, Hobart.

Davis, J. R. (2000). ASM Specialty Handbook: Nickel, Cobalt, and Their Alloys. Ohio, Ohio: ASM International.

Diaz, C., Landolt, C., Vahed, A., Warner, A., & Taylor, J. (1988). A Review of Nickel Pyrometallurgical Operation. JOM. 40. 10.1007/BF03258548.

Elias, M., (2002). *Nickle laterite deposits-geological overview, resources and exploitation, in giant ore deposit: characteristics, genesis and exploration*. Centre Ore Deposit Res., Univ. Tasmania, Spec. Pub. 4, 205–220.

Evans, A.M., (1993). *Ore Geology and Industrial Minerals*. *Blackwell Scientific Publications*, Oxford, P 390.

Farrokhpay, S. and Filippov, L. (2016). Challenges in processing nickel laterite ores by flotation. Intl. Journal of Mineral Processing. vol. 151, pp. 59-67.

Gleeson, S., Butt, C. & El, M., (2003). Nickel Laterites : A Review. Society of Economic Geologists (SEG), July, pp. 12-18.

Golightly, J.P., (1981). *Nickeliferous laterite deposits*. In: Economic Geology, 75th Anniversary Volume, pp. 710–735.

Hannis, S.; & Bide, T. (2009). *Mineral Profile Cobalt*. Nottingham, England, United Kingdom: British Geological Survey.

Husain, A., Nur, I., Sufriadin. (2018). Karakteristik Mineralogi dan Geokimia Bijih Nikel Laterit di Bukit Hasan, PT. Vale Indonesia Tbk, Sulawesi Selatan: Implikasinya Terhadap Pengolahan. Makassar: Universitas Hasanuddin.

Juvelyn S.D., Amparado R.F., Malaluan R.M., Demayo C.G. (2012). Characterization and Leaching Assesment of Ferronickel Slag from a Smelting Plant ini Iligan City Philippines,International Journal of Environmental Science and Development, 3(5): 470- 474

Kadarusman, A., (2001). *Geodynamic of Indonesian region; a petrological Approaches*, unpublished PhD Thesis, Tokyo Institute ofTechnology, 456p.

Kadarusman, A., Miyashita, S., Maruyama, S. & Parkinson, (2004). Petrology, Geochemistry and Paleogeographic Reconstruction of the East Sulawesi Ophiolite, Indonesia. Tectonophysics, Volume 392, pp. 55-83.

Kursunoglu, S., Kaya, M. (2016). Atmospheric Pressure Acid Leaching Of Caldag Lateritic Nickel Ore. International Journal of Mineral Processing. Vol. 150. Pp. 1 – 8.

Kyle, J. (2010). Nickel laterite processing technologies – where to next? Paper presented at the ALTA 2010 Nickel/Cobalt/Copper Conference, Perth.

Pan, C.X.Lv., BaiC., LiuX. D.Li, MinJ. (2013). Meltingfeaturesand viscosityOfSi-O2-CaO- MGOAl2O3-feOnickelslag inlateritemetallurgy. J. Min. Metall. Sect. B-Metall. 49(1)B: 9-12.

Prasetyo, P.; & Ronald, N. (2011). Masih Terbukanya Peluang Penelitian Proses Caron Untuk Mengolah Nikel Laterit Kadar Rendah Di Indonesia. Majalah Metalurgi Vol. 26. Hal, 35-44.

PT Vale Indonesia Tbk. (2018). Laporan Tahunan 2018 “Dedicating Through Ages, Optimizing Oppurtunities”. Jakarta.

Saefuddin Sarief. (1989). Konservasi Tanah Dan Air. Bandung : C. V. Pustaka Buana.

Setiawan, I. (2016). Pengolahan Nikel Laterit Secara Pirometalurgi: Kini Dan Penelitian Kedepan. Paper presented at the Seminar Nasional Sains dan Teknologi 2016 Yogyakarta.

Sharma, A., & Adikari, S. B. (2018). Marketing Pattern Of Rubber Plantation In Tripura. International Journal Of Current Microbiology And Applied Sciences, 7(06), 847–853. Https://Doi.Org/10.20546/Ijcmas.2018.706.099.

Sheik, A., Ghosh, M., Sanjay, K., Subbaiah, T., Mishra, K., (2013). Dissolution kinetics of nickel from spent catalyst in nitric acid medium. J. Taiwan Inst. Chem. Eng. 44, 34–39.

Solihin. (2012). Pengolahan bijih nikel kadar rendah untuk mendukung industri baja tahan karat, Jakarta: LIPI.

Stopić, R., Friedrich, G. (2016). Hydrometallurgical Processing Of Nickel Lateritic Ores. Vojnotehnički Glasnik/Military Technical Courier Vol. 64. Pp. 1033-1047.

Sufriadin, (2013). *Mineralogi, Geokimia dan Sifat Leaching pada Endapan Nikel dan Kalsin Nikel Laterit*, Majalah Metalurgi 2015, Pp 71-80

Sufriadin, Pramumijoyo, I., Warmada, S. & Imai, I. (2011). Study on Mineralogy and Chemistry of the Saprolitic Nickel ore from Soroako, Sulawesi, Indonesia: Implication for the Lateritic Ore Processing. Journal of South east Asian Applied Geology, 3(1), p. 23–33.

Superiadi, A. (2006). The Key Role Of Mineralogy and Ore Chemistry In Optimizing Metallurgical Process of Nickel Laterite. In Proceedings PIT IAGI Riau. Pp. 1-12.

Supriyatna, Y. I., Sihotang, I. H. And Sudibyo. (2019). Preliminary Study of Smelting of Indonesian Nickel Laterite Ore Using an Electric Arc Furnace. In The 6th International Conference on Advanced Materials Science and Technology 2018, 6th ICAMST (pp. 127-131).

Tonggiroh, A. (2019). Dasar – dasar Geokimia Eksplorasi. Makassar: CV. Social Politic Genius (SIGn).

Trescases, J. J., (1975). *Levolution Geochimique Supergene des Roches Ultrabasiques en Zone Tropicale; Formations des Gisements Nickeliferes de Nouvelle-Caledonie.* Paris, ORSTOM Mem. 78.

UBP Nikel Maluku Utara. (2013). Instruksi kerja PT. ANTAM Tbk. UBP Nikel Maluku Utara yaitu IK09.276.21.R01. Buli : PT. ANTAM Tbk

Villanova-de-Benavent, C., Proenza, J. A., Galí, S., García-Casco, A., Tauler, E., Lewis, J. F., Longo, F., (2014). Garnierites and Garnierites: Textures, Mineralogy and Geochemistry of Garnierites in the Falcondo Ni-laterite

Deposit, Dominican Republic. Ore Geology Reviews, Volume 58, pp. 91-109.

Widi A., Zulfiadi Z., Achmad S., Kusno I., Fajar N., dan Erik P. (2012). Pembuatan Nickel Pig Iron dari Bijih Nikel Laterit Indonesia Menggunakan Mini Blast Furnace. Prosiding InsINas MT66-71, 0404.

Winarno, T., Rinal, K. Ali., Resa Komala. (2022). Hubungan Ukuran Butir Terhadap Kadar Nikel pada Zona Saprolit Endapan Nikel Laterit Site Moronopo, Kabupaten Halmahera Timur, Maluku Utara. http://ejournal.undip.ac.id/index.php/teknik, 43 (1), 2022, 87-92.

Zhu, D.Q., Cui, Y., Vining, K., Hapugoda, S., Douglas, J., Pan, J., & Zheng, G.L., (2012). Upgrading low nickel content laterite ores using selective reduction followed by magnetic separation. Elsevier International Journal of Mineral Processing, Australia.

Lampiran 1 Data Analisis XRD SA-LIM

Match! Phase Analysis Report

Sample: LIM-SA (5-70)

Sample Data

File name	LIM-SA.ORG
File path	C:/Users/alfia/Desktop/alfian/LIM-SA
Data collected	May 8, 2023 19:22:51
Data range	5.000° - 70.000°
Original data range	5.000° - 70.000°
Number of points	3251
Step size	0.020
Rietveld refinement converged	No
Alpha2 subtracted	No
Background subtr.	No
Data smoothed	Yes
Radiation	X-rays
Wavelength	1.540600 Å

Analysis Results

Phase composition (Weight %)

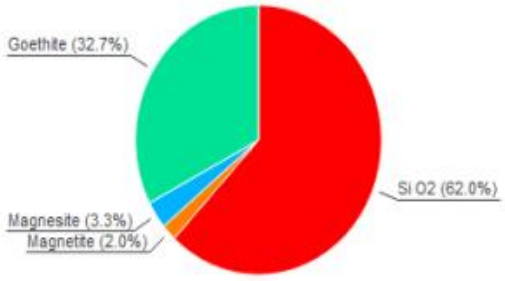

Elemental composition (Weight %)

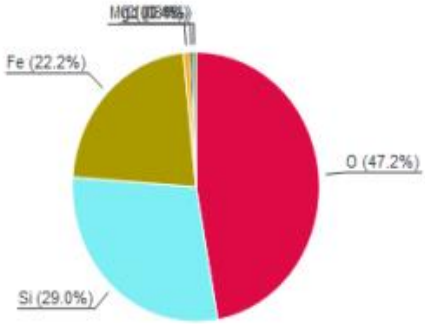

Index	*Amount (%)*	*Name*	*Formula sum*
A	62.0	Si O2	O2 Si
B	2.0	Magnetite	Fe3 O4
C	3.3	Magnesite	C Cd0.1 Mg0.9 O3
D	32.7	Goethite	Fe O2
	11.6	*Unidentified peak area*	

Amounts calculated by RIR (Reference Intensity Ratio) method

Element	*Amount (weight %)*
O	*47.2%(*)*
Si	29.0%
Fe	22.2%
Mg	0.8%
C	*0.4%(*)*
Cd	0.4%
**LE (sum)*	*47.6%*

Details of identified phases

A: Si O2 (62.0 %)*

Formula sum	O2 Si
Entry number	96-152-6861
Figure-of-Merit (FoM)	0.825045*
Total number of peaks	70
Peaks in range	18
Peaks matched	18
Intensity scale factor	1.05*
Space group	P 31 2 1
Crystal system	trigonal (hexagonal axes)
Unit cell	a= 4.9019 Å c= 5.3988 Å
I/Ic	2.92
Calc. density	2.664 g/cm³
Reference	Tucker M.G., Dove M.T., Keen D.A., "A detailed structural characterization of quartz on heating through thealpha - beta transition", Mineralogical Magazine (1969-) **65**, 489-507 (2001)

B: Magnetite (2.0 %)*

Formula sum	Fe3 O4
Entry number	96-900-2326
Figure-of-Merit (FoM)	0.702060*
Total number of peaks	34
Peaks in range	11
Peaks matched	11
Intensity scale factor	0.07*
Space group	F d -3 m
Crystal system	cubic
Unit cell	a= 8.2321 Å
I/Ic	5.67
Calc. density	5.514 g/cm³
Reference	Haavik C., Stolen S., Fjellvag H., Hanfland M., Hausermann D., "Equation of state of magnetite and its high-pressure modification:Thermodynamics of the Fe-O system at high pressureSample at P = 15.7 GPa", American Mineralogist **85**, 514-523 (2000)

C: Magnesite (3.3 %)*

Formula sum	C Cd0.1 Mg0.9 O3
Entry number	96-901-0226
Figure-of-Merit (FoM)	0.673650*
Total number of peaks	69
Peaks in range	17
Peaks matched	15
Intensity scale factor	0.04*
Space group	R -3 c
Crystal system	trigonal (hexagonal axes)
Unit cell	a= 4.6638 Å c= 15.1720 Å
I/Ic	2.08
Calc. density	3.246 g/cm³
Reference	Bromiley F. A., Boffa Ballaran T., Langenhorst F., Seifert F., "Order and miscibility in the otavite - magnesite solid solutionLocality: syntheticSample: X_Mg = .9, synthesized at 800 C, 1 GPa, 1 h", American Mineralogist **92**, 829-836 (2007)

D: Goethite (32.7 %)*

Formula sum	Fe O2
Entry number	96-901-5697
Figure-of-Merit (FoM)	0.785484*
Total number of peaks	183
Peaks in range	40
Peaks matched	39
Intensity scale factor	0.60*
Space group	P b n m
Crystal system	orthorhombic
Unit cell	a= 4.6188 Å b= 9.9528 Å c= 3.0236 Å
I/Ic	3.17
Calc. density	4.198 g/cm³
Reference	Hazemann J.-L., Bérar J. F., Manceau A., "Rietveld studies of the aluminium-iron substitution in synthetic goethite", Materials Science Forum **79-82**, 821-826 (1991)

(*)2theta values have been shifted internally for the calculation of the amounts, the intensity scaling factors as well as the figure-of-merit (FoM), due to the active search-match option 'Automatic zero point adaption'.

Candidates

Name	*Formula*	*Entry No.*	*FoM*
Silicon carbide (Moissanite 3C)	C Si	96-101-1032	0.7356
Ta N	N Ta	96-231-0958	0.7349
Periclase	Mg O	96-900-6778	0.7254
Fe.914 O	Fe0.914 O	96-154-1152	0.7243
Manganese-delta	Mn	96-900-8592	0.7221
Periclase	Mg O	96-900-6475	0.7195
(Ge0.16 Pd0.84)	Ge0.16 Pd0.84	96-152-3553	0.7177
(Nb7 Ti3 N10)0.4	N4 Nb2.8 Ti1.2	96-153-9369	0.7155
Si C N	C N Si	96-154-1620	0.7140
(Sn0.1 V0.9)	Sn0.1 V0.9	96-152-7759	0.7132
Periclase	Mg O	96-900-6474	0.7088
Periclase	Mg O	96-900-6768	0.7031
(Au0.5 Pd0.5) Zn	Au0.5 Pd0.5 Zn	96-151-0286	0.6844
(Os0.5 Re0.5) Ti	Os0.5 Re0.5 Ti	96-152-3515	0.6824
Disodium praseodymium(IV) oxide	Na5.34 O8.01 Pr2.67	96-101-0654	0.6821
(Ir0.62 Re0.38) Ti	Ir0.62 Re0.38 Ti	96-152-3518	0.6806
	Ag Zn	96-150-9568	0.6782
Co2 (Nb Sn)	Co2 Nb Sn	96-152-7186	0.6754
	Os Ti	96-153-7946	0.6723
	Nb Ni2 Sn	96-153-9317	0.6713
	Cu2 Zn Zr	96-152-4553	0.6709
(Fe0.65 Pt0.35)	Fe0.65 Pt0.35	96-152-3355	0.6687
	Cu2 Mn Sn	96-230-0522	0.6679
(Ti0.89 V0.11)	Ti0.89 V0.11	96-152-7833	0.6655

	Cu2 In Mn	96-152-4977	0.6636
Zinc cadmium tin(IV) oxide (1.8/.2/1/4)	Cd0.2 O4 Sn Zn1.8	96-100-1189	0.6617
Mn Fe1.2 In.8 O4	Fe1.2 In0.8 Mn O4	96-153-8484	0.6604
	Cd O4 Rh2	96-432-9526	0.6543
(Mo0.33 Re0.33 V0.34)	Mo0.33 Re0.33 V0.34	96-152-2927	0.6542
	Cu2 Mn Sn	96-591-0005	0.6537
Calcium	Ca	96-901-2917	0.6533
	Cu2 Ga Sc	96-152-4877	0.6526
	Hg3 Zr	96-152-2701	0.6502
	Nb Ni2 Sn	96-153-9561	0.6488
Yb Ni0.39 Sb	Ni0.39 Sb Yb	96-722-2621	0.6477
	Co2 Nb Sn	96-152-5520	0.6472
	Sb Tb	96-900-8739	0.6455
Tb Sb	Sb Tb	96-153-7717	0.6448
Potassium aluminium silicate hydroxide * (Muscovite 2M1)	Al3 H2 K O12 Si3	96-101-1050	0.6439
Potassium aluminium silicate hydroxide * (Muscovite 2M1)	Al3 H2 K O12 Si3	96-110-0014	0.6439
Er Bi	Bi Er	96-153-9424	0.6438
	Cl K0.8 Na0.2	96-900-3168	0.6434
Periclase	Mg O	96-900-6777	0.6433
	Cl K0.8 Na0.2	96-900-3177	0.6431
Pb Sn Se Te	Pb0.8 Se1.2 Sn1.2 Te0.8	96-153-8840	0.6429
	Cl K0.8 Na0.2	96-900-3174	0.6426
(Pd0.81 Zn0.19)	Pd0.81 Zn0.19	96-152-2607	0.6425
	Cl K0.8 Na0.2	96-900-3162	0.6424
	Cl K0.8 Na0.2	96-900-3157	0.6416
Sylvite	Cl K	96-900-3128	0.6414
	Cl K0.8 Na0.2	96-900-3145	0.6413
Neon	Ne	96-901-1722	0.6412

and 153 others...

Search-Match

Settings

Reference database used	COD-Inorg 2022.11.07
Automatic zeropoint adaptation	Yes
Downgrade entries with low scaling factors	Yes
Minimum figure-of-merit (FoM)	0.60
2theta window for peak corr.	0.30 deg.
Minimum rel. int. for peak corr.	0
Parameter/influence 2theta	0.50
Parameter/influence intensities	0.50
Parameter multiple/single phase(s)	0.50

Peak List

No.	*2theta [°]*	*d [Å]*	*I/I0 (peak height)*	*Counts (peak area)*	*FWHM*	*Matched*
1	6.94	12.7268	7.40	0.10	0.0232	
2	9.44	9.3612	12.36	0.17	0.0232	
3	10.44	8.4667	17.23	2.16	0.2158	
4	10.46	8.4505	16.75	3.98	0.4084	
5	10.96	8.0661	14.07	2.38	0.2907	
6	11.22	7.8798	15.39	2.08	0.2319	
7	11.88	7.4435	6.55	0.47	0.1226	
8	12.22	7.2371	25.73	2.10	0.1400	
9	12.80	6.9104	19.48	5.63	0.4970	
10	13.46	6.5730	12.33	2.40	0.3351	
11	14.44	6.1291	16.30	1.33	0.1400	
12	14.96	5.9172	13.88	1.13	0.1400	
13	15.32	5.7789	9.08	0.74	0.1400	
14	15.74	5.6257	6.21	1.49	0.4110	
15	16.20	5.4670	6.73	1.98	0.5245	
16	17.52	5.0579	12.71	4.72	0.6380	
17	17.78	4.9845	18.36	4.34	0.4065	D
18	17.98	4.9295	15.27	2.59	0.2907	
19	18.70	4.7413	59.99	6.11	0.1750	B
20	19.74	4.4938	18.22	1.48	0.1400	
21	19.94	4.4492	9.02	0.74	0.1400	
22	20.90	4.2469	365.15	72.42	0.3407	A
23	21.36	4.1565	172.19	64.15	0.6400	D
24	22.02	4.0334	41.86	15.59	0.6400	
25	23.10	3.8472	15.80	5.89	0.6400	
26	23.94	3.7141	6.70	2.49	0.6400	
27	24.88	3.5759	6.81	2.54	0.6400	C
28	25.76	3.4557	9.45	3.52	0.6400	
29	26.02	3.4217	60.57	4.94	0.1400	D
30	26.70	3.3361	1000.00	138.34	0.2377	A
31	27.70	3.2179	5.26	3.08	1.0043	
32	28.98	3.0786	6.54	3.82	1.0043	
33	30.26	2.9512	15.27	8.93	1.0043	
34	30.86	2.8952	9.16	5.35	1.0043	B
35	31.68	2.8221	6.36	3.72	1.0043	

36	32.02	2.7929	8.07	4.72	1.0043	
37	32.38	2.7627	16.70	9.77	1.0043	C
38	33.24	2.6931	85.05	49.72	1.0043	D
39	34.24	2.6167	21.75	12.72	1.0043	
40	34.84	2.5730	62.14	36.33	1.0043	D
41	35.64	2.5171	56.54	33.05	1.0043	C,D
42	35.92	2.4981	55.27	32.31	1.0043	D
43	36.26	2.4755	137.00	28.71	0.3600	B
44	36.68	2.4481	344.67	80.25	0.4000	A,D
45	37.54	2.3939	30.42	7.08	0.4000	
46	38.10	2.3600	16.77	3.90	0.4000	B
47	38.50	2.3364	11.51	2.68	0.4000	C
48	38.82	2.3179	8.75	2.04	0.4000	D
49	39.54	2.2773	70.83	16.49	0.4000	A
50	39.98	2.2533	41.63	9.69	0.4000	D
51	40.36	2.2329	86.42	20.12	0.4000	A
52	41.14	2.1924	44.49	10.36	0.4000	D
53	41.38	2.1802	52.92	12.32	0.4000	
54	42.52	2.1244	150.85	18.64	0.2122	A,C
55	42.96	2.1036	7.17	0.89	0.2122	
56	43.28	2.0888	13.13	1.62	0.2122	D
57	43.50	2.0788	10.51	1.30	0.2122	
58	43.80	2.0652	4.30	0.53	0.2122	
59	44.08	2.0527	13.03	1.61	0.2122	B
60	44.56	2.0317	7.14	0.88	0.2122	
61	44.96	2.0146	8.38	1.04	0.2122	D
62	45.36	1.9977	13.35	1.09	0.1400	
63	45.86	1.9771	58.29	8.00	0.2357	A
64	46.68	1.9443	7.56	1.04	0.2357	C
65	46.94	1.9341	24.79	2.02	0.1400	
66	47.50	1.9126	19.82	5.10	0.4424	D
67	48.18	1.8872	13.26	3.41	0.4424	B,D
68	48.50	1.8755	10.32	2.66	0.4424	
69	48.88	1.8618	7.78	2.00	0.4424	
70	49.34	1.8455	9.03	2.33	0.4424	
71	50.22	1.8152	133.88	21.55	0.2765	A
72	50.78	1.7965	33.69	5.42	0.2765	A,D
73	51.28	1.7802	13.49	2.17	0.2765	C
74	51.54	1.7718	17.57	2.83	0.2765	D
75	52.00	1.7572	13.67	1.11	0.1400	
76	52.78	1.7330	27.81	10.75	0.6640	
77	53.28	1.7180	69.12	26.72	0.6640	C,D
78	53.52	1.7108	77.33	29.89	0.6640	C
79	54.06	1.6950	38.99	15.07	0.6640	D
80	54.58	1.6801	29.13	11.26	0.6640	B
81	54.94	1.6699	47.77	18.46	0.6640	A
82	55.38	1.6577	22.29	8.62	0.6640	A,D
83	56.00	1.6408	8.91	3.44	0.6640	
84	56.22	1.6349	4.24	1.64	0.6640	
85	57.32	1.6061	18.19	7.03	0.6640	A,D
86	57.90	1.5914	16.03	6.20	0.6640	B
87	58.94	1.5658	44.23	17.10	0.6640	D
88	59.14	1.5609	44.86	17.34	0.6640	D
89	60.02	1.5401	169.03	25.76	0.2618	A
90	60.64	1.5259	6.38	0.97	0.2618	D
91	61.48	1.5070	36.39	10.23	0.4829	D
92	61.96	1.4965	21.77	6.12	0.4829	C
93	62.60	1.4827	5.29	1.49	0.4829	
94	62.96	1.4751	22.11	6.22	0.4829	D
95	63.24	1.4692	12.33	3.46	0.4829	D
96	63.76	1.4585	25.58	7.19	0.4829	
97	63.96	1.4544	30.88	8.68	0.4829	B,D
98	64.20	1.4496	34.45	9.68	0.4829	A,D
99	64.58	1.4420	16.81	4.73	0.4829	
100	65.44	1.4251	6.62	1.86	0.4829	
101	65.70	1.4201	10.38	2.92	0.4829	C,D
102	65.96	1.4151	20.53	5.77	0.4829	A,C
103	67.04	1.3949	22.55	1.84	0.1400	B,D
104	67.48	1.3869	24.22	1.97	0.1400	D
105	67.76	1.3818	53.77	12.00	0.3833	C,D
106	67.94	1.3786	50.21	11.20	0.3833	A
107	68.36	1.3711	104.99	23.43	0.3833	A,B,C,D
108	69.12	1.3579	20.78	4.64	0.3833	D
109	69.72	1.3477	8.63	1.93	0.3833	C,D

Integrated Profile Areas

Based on calculated profile

Profile area	*Counts*	*Amount*
Overall diffraction profile	69368	100.00%

Background radiation	31497	45.41%
Diffraction peaks	37871	54.59%
Peak area belonging to selected phases	29832	43.01%
Peak area of phase A (Si O2)	*12518*	*18.05%*
Peak area of phase B (Magnetite)	*903*	*1.30%*
Peak area of phase C (Magnesite)	*494*	*0.71%*
Peak area of phase D (Goethite)	*15917*	*22.95%*
Unidentified peak area	8039	11.59%

Peak Residuals

Peak data	***Counts***	***Amount***
Overall peak intensity	1168	100.00%
Peak intensity belonging to selected phases	1073	91.83%
Unidentified peak intensity	95	8.17%

Diffraction Pattern Graphics

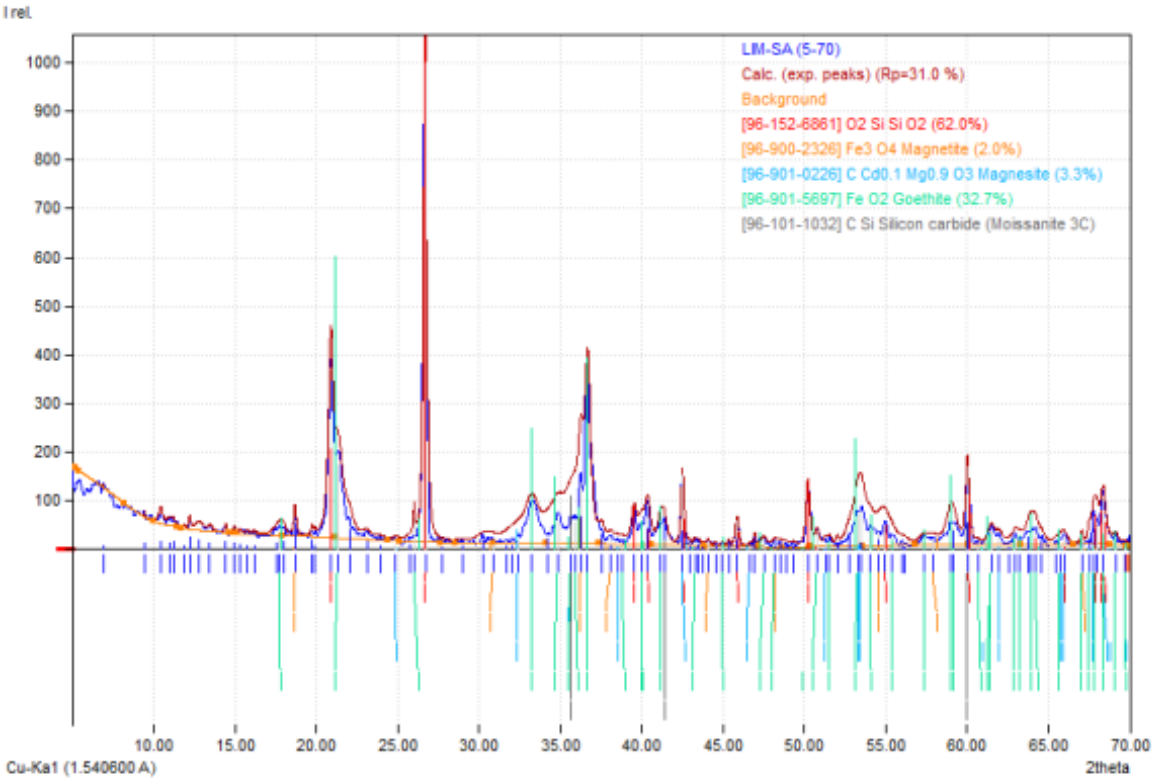

Lampiran 2 Data Analisis XRD SA-SAP

Match! Phase Analysis Report

Sample: SAP-SA (5-70)

Sample Data

File name	SAP-SA.ORG
File path	C:/Users/alfia/Desktop/alfian/SAP-SA
Data collected	May 8, 2023 19:22:52
Data range	5.000° - 70.000°
Original data range	5.000° - 70.000°
Number of points	3251
Step size	0.020
Rietveld refinement converged	No
Alpha2 subtracted	No
Background subtr.	No
Data smoothed	Yes
Radiation	X-rays
Wavelength	1.540600 Å

Analysis Results

Phase composition (Weight %)

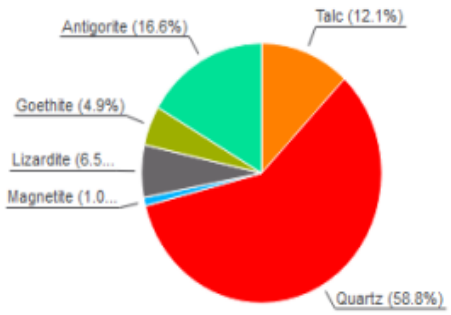

Elemental composition (Weight %)

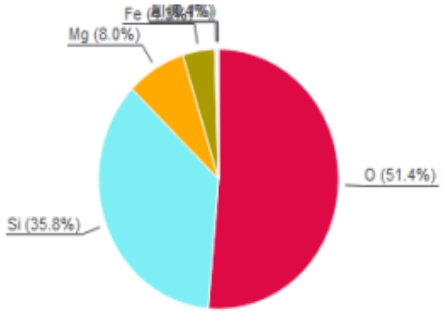

Index	*Amount (%)*	*Name*	*Formula sum*
A	12.1	Talc	H2 Mg3 O12 Si4
B	58.8	Quartz	O2 Si
C	1.0	Magnetite	Fe3 O4
D	6.5	Lizardite	Al0.201 Fe0.339 H4 Mg2.544 O9 Si1.904
E	4.9	Goethite	Fe O2
F	16.6	Antigorite	H58 Mg45 O138 Si32
	23.6	*Unidentified peak area*	

Element	*Amount (weight %)*
O	*51.4%(*)*
Si	35.8%
Mg	8.0%
Fe	4.3%
H	*0.4%(*)*
Al	0.1%
**LE (sum)*	*51.8%*

Amounts calculated by RIR (Reference Intensity Ratio) method

Details of identified phases

A: Talc (12.1 %)*

Formula sum	H2 Mg3 O12 Si4
Entry number	96-900-8298
Figure-of-Merit (FoM)	0.735388*
Total number of peaks	251
Peaks in range	186
Peaks matched	168
Intensity scale factor	0.07*
Space group	C -1
Crystal system	triclinic (anorthic)
Unit cell	a= 5.2900 Å b= 9.1730 Å c= 9.4600 Å α= 90.460° β= 98.680 ° γ= 90.090 °
I/Ic	1.03
Calc. density	2.776 g/cm³
Reference	Perdikatsis B., Burzlaff H., "Strukturverfeinerung am talk Mg3[(OH)2Si4O10]", Zeitschrift fur Kristallographie **156**, 177-186 (1981)

B: Quartz (58.8 %)*

Formula sum	O2 Si
Entry number	96-901-0145
Figure-of-Merit (FoM)	0.832009*
Total number of peaks	71
Peaks in range	18
Peaks matched	18
Intensity scale factor	1.00*
Space group	P 32 2 1 S
Crystal system	trigonal (hexagonal axes)
Unit cell	a= 4.9230 Å c= 5.4090 Å
I/Ic	2.86
Calc. density	2.636 g/cm³
Reference	Ikuta D., Kawame N., Banno S., Hirajima T., Ito K., Rakovan J. F., Downs R. T., Tamada O., "First in situ X-ray diffraction identification of coesite and retrogradequartz on a glass thin section of an ultrahigh-pressure metamorphic rock andtheir crystal structure details Locality: Yangkou meta-igneous complex in themiddle part of the Sulu UHP terrain, eastern China Note: Sample is on a thinsection", American Mineralogist **92**, 57-63 (2007)

C: Magnetite (1.0 %)*

Formula sum	Fe3 O4
Entry number	96-900-5815
Figure-of-Merit (FoM)	0.673462*
Total number of peaks	36
Peaks in range	11
Peaks matched	9
Intensity scale factor	0.04*
Space group	F d -3 m
Crystal system	cubic
Unit cell	a= 8.3390 Å
I/Ic	5.86
Calc. density	5.304 g/cm³
Reference	Finger L. W., Hazen R. M., Hofmeister A. M., "High-pressure crystal chemistry of spinel (MgAl2O4)and magnetite (Fe3O4): comparisons with silicate spinelsSample: P = 26 kbar", Physics and Chemistry of Minerals **13**, 215-220 (1986)

D: Lizardite (6.5 %)*

Formula sum	Al0.201 Fe0.339 H4 Mg2.544 O9 Si1.904
Entry number	96-901-6051
Figure-of-Merit (FoM)	0.686217*
Total number of peaks	114
Peaks in range	28
Peaks matched	26
Intensity scale factor	0.06*
Space group	P 3 1 m
Crystal system	trigonal (hexagonal axes)
Unit cell	a= 5.3263 Å c= 7.2885 Å
I/Ic	1.48
Calc. density	2.668 g/cm³
Reference	Laurora A., Brigatti M. F., Malferrari D., Galli E., "The crystal chemistry of lizardite-1T from northApennines ophiolites near Modena, ItalyNote: sample Santa Scolastica, polytype 1T", The Canadian Mineralogist **49**, 1045-1054 (2011)

E: Goethite (4.9 %)*

Formula sum	Fe O2
Entry number	96-901-1413
Figure-of-Merit (FoM)	0.710906*
Total number of peaks	187
Peaks in range	38
Peaks matched	34
Intensity scale factor	0.08*
Space group	P b n m
Crystal system	orthorhombic
Unit cell	a= 4.5900 Å b= 10.0000 Å c= 3.0300 Å
I/Ic	2.85
Calc. density	4.195 g/cm³
Reference	Hoppe W., "Uber die kristallstruktur von alpha-AlOOH (diaspore) und alpha-FeOOH(nadeleisenerz) Locality: Synthetic", Zeitschrift fur Kristallographie **103**, 73-89 (1940)

F: Antigorite (16.6 %)*

Formula sum	H58 Mg45 O138 Si32
Entry number	96-900-4000
Figure-of-Merit (FoM)	0.750215*
Total number of peaks	327
Peaks in range	327
Peaks matched	259
Intensity scale factor	0.07*
Space group	C 1 2/m 1
Crystal system	monoclinic

Unit cell	a= 81.6640 Å b= 9.2550 Å c= 7.2610 Å β= 91.409 °
I/Ic	0.70
Calc. density	2.578 g/cm³
Reference	Capitani G. C., Mellini M., "The crystal structure of a second antigorite polysome (m = 16),by single-crystal synchrotron diffraction", American Mineralogist **91**, 394-399 (2006)

(*)2theta values have been shifted internally for the calculation of the amounts, the intensity scaling factors as well as the figure-of-merit (FoM), due to the active search-match option 'Automatic zero point adaption'.

Candidates

Name	*Formula*	*Entry No.*	*FoM*
Neon	Ne	96-901-1634	0.7177
Eu Rh3 B2	B2 Eu Rh3	96-151-0676	0.7013
Lime	Ca O	96-900-6731	0.7007
Alabandite	Mn S	96-900-5943	0.7000
Lime	Ca O	96-900-6742	0.6987
Lime	Ca O	96-900-6743	0.6980
	Fe4 O5	96-155-1316	0.6975
Ti H2	H2 Ti	96-403-1667	0.6945
Hf Ta N2	Hf N2 Ta	96-153-8054	0.6926
Ag2.88 S I	Ag2.88 I S	96-150-9750	0.6909
Lime	Ca O	96-900-6730	0.6903
Silver sulfide - $-alpha (Argentite)	Ag2 S	96-101-1338	0.6880
(U Zr)	U Zr	96-152-3848	0.6825
(Sr0.92 Eu0.08) Cu O2.03	Cu Eu0.08 O2.03 Sr0.92	96-152-5870	0.6818
Silver selenide - $-alpha	Ag2 Se	96-101-1339	0.6814
Zr3 V3 B0.372 O0.558 D5.944	B0.372 D5.944 O0.558 V3 Zr3	96-152-7022	0.6813
	Mo N2 O9 P2	96-901-4933	0.6809
(Zn0.914 Li0.086) O0.957	Li0.086 O0.957 Zn0.914	96-152-7032	0.6801
{[4-Br-3,5-(CF3)2Pz]Cu}3	C15 Br3 Cu3 F18 N6	96-433-6872	0.6784
	C Hf	96-900-8642	0.6763
Manganese sulfide (Alabandite)	Mn S	96-101-1352	0.6752
	Al2 O	96-412-4784	0.6751
	La Mo Na O4	96-200-0341	0.6749
Alabandite	Mn S	96-900-5944	0.6745
neodymium manganese copper phosphide (2/3/9/7)	Cu9 Mn3 Nd2 P7	96-433-3629	0.6728
	Hg Ti	96-152-2698	0.6724
	C46 Al2 F72 I3 Mo3 O22	96-155-7539	0.6708
Lime	Ca O	96-900-6728	0.6707
Fe2 (Ti0.2 Zr0.8)	Fe2 Ti0.2 Zr0.8	96-152-3276	0.6699
Titanium nitride - \d	N Ti2	96-110-0031	0.6694
Titanium nitride - \d	N Ti2	96-110-1043	0.6694
	N0.5 Ti	96-901-5030	0.6694
{NH(proI)3}[MnCr(ox)3](H2O)2	C15 H26 Cr Mn N O17	96-410-5047	0.6685
(syn-rac)-trans-Dichloro-(5,7,7,12,14,14-hexamethyl-1,4,8,11-tetraazacyclo-tetradeca-4,11-diene)-cobalt(iii) perchlorate	C16 Cl3 Co N4 O4	96-210-3784	0.6684
(Fe0.91 Ga0.09)2 Sc	Fe1.82 Ga0.18 Sc	96-152-4397	0.6678
Metaschoepite	H34 Na0.47 O37.082 U8	96-901-0199	0.6673
	Fe2 Sc	96-152-3285	0.6671
Alabandite	Mn S	96-900-5931	0.6669
Bis(ammonium) molybdenyl diphosphate	H8 Mo N2 O9 P2	96-100-8371	0.6666
(Co Ni) U	Co Ni U	96-152-5512	0.6661
(Cd Mg3)0.5	Cd0.5 Mg1.5	96-152-5130	0.6658
(Cu0.255 Zn0.745)	Cu0.255 Zn0.745	96-152-5235	0.6654
	Ag2 Cu2 O3	96-150-9786	0.6652
Metaschoepite	H34 Na0.48 O37.91 U8	96-901-0195	0.6651
Umohoite	H4 Mo O8 U	96-900-4564	0.6646
	Au2 In Y	96-151-0437	0.6645
Alabandite	Mn S	96-900-8676	0.6645
(Mg0.97 Zn0.03)	Mg0.97 Zn0.03	96-152-2394	0.6643
(U O2) ((Mo O4) (H2 O)) (H2 O)1.45	H4.9 Mo O8.45 U	96-152-1823	0.6641
Zr3 V3 B0.2 O0.3 D8.88	B0.2 D8.88 O0.3 V3 Zr3	96-152-7023	0.6641
	Co2 Pu	96-152-4239	0.6636
	C6 Cl3 N3 O6	96-200-1647	0.6633

and 1443 others...

Search-Match

Settings

Reference database used	COD-Inorg 2022.11.07
Automatic zeropoint adaptation	Yes
Downgrade entries with low scaling factors	Yes
Minimum figure-of-merit (FoM)	0.60
2theta window for peak corr.	0.30 deg.
Minimum rel. int. for peak corr.	0
Parameter/influence 2theta	0.50
Parameter/influence intensities	0.50
Parameter multiple/single phase(s)	0.50

Peak List

No.	*2theta [°]*	*d [Å]*	*I/I0 (peak height)*	*Counts (peak area)*	*FWHM*	*Matched*

1	6.34	13.9298	15.83	0.98	0.0959	
2	6.64	13.3011	26.11	2.38	0.1413	F
3	6.88	12.8376	31.39	2.86	0.1413	
4	7.16	12.3362	23.45	2.14	0.1413	
5	7.68	11.5021	12.02	0.95	0.1223	
6	8.54	10.3456	11.55	0.77	0.1031	F
7	8.80	10.0405	9.17	0.61	0.1031	
8	9.08	9.7315	8.88	0.59	0.1031	
9	9.46	9.3415	7.88	0.61	0.1200	A
10	9.68	9.1296	8.19	0.51	0.0970	F
11	9.96	8.8736	5.42	0.34	0.0970	F
12	10.52	8.4025	7.09	0.55	0.1200	
13	10.76	8.2156	16.31	1.82	0.1733	F
14	10.96	8.0661	12.10	1.35	0.1733	F
15	11.16	7.9220	13.75	1.06	0.1200	
16	11.50	7.6885	21.86	4.85	0.3443	
17	12.08	7.3207	114.98	25.52	0.3443	D,F
18	12.32	7.1786	107.11	23.78	0.3443	F
19	12.76	6.9320	9.91	2.20	0.3443	F
20	13.08	6.7631	2.54	0.56	0.3443	F
21	13.34	6.6319	10.40	2.31	0.3443	
22	13.58	6.5152	11.56	2.57	0.3443	F
23	14.00	6.3207	8.42	1.87	0.3443	F
24	14.24	6.2147	4.59	1.02	0.3443	
25	14.68	6.0294	8.35	1.85	0.3443	F
26	14.92	5.9330	9.70	2.15	0.3443	F
27	15.38	5.7565	7.55	1.67	0.3443	F
28	15.84	5.5904	4.84	1.07	0.3443	F
29	16.36	5.4138	8.35	1.85	0.3443	F
30	17.14	5.1692	14.33	3.18	0.3443	F
31	17.88	4.9569	11.72	2.60	0.3443	E,F
32	18.30	4.8441	12.54	2.78	0.3443	F
33	18.52	4.7870	14.86	3.30	0.3443	C,F
34	18.76	4.7263	17.63	3.91	0.3443	
35	18.96	4.6769	21.18	4.70	0.3443	A,F
36	19.20	4.6190	33.67	7.47	0.3443	D,F
37	19.42	4.5671	48.97	10.87	0.3443	A,F
38	19.62	4.5210	57.84	12.84	0.3443	A,F
39	20.04	4.4272	56.99	12.65	0.3443	F
40	21.00	4.2269	194.57	70.25	0.5600	B,F
41	21.54	4.1222	80.37	29.02	0.5600	A,E,F
42	21.84	4.0662	51.30	18.52	0.5600	F
43	22.22	3.9975	34.28	12.38	0.5600	F
44	22.50	3.9484	26.99	9.75	0.5600	
45	22.92	3.8770	28.69	10.36	0.5600	A,D,F
46	23.20	3.8309	19.80	7.15	0.5600	F
47	23.44	3.7922	19.86	7.17	0.5600	F
48	23.76	3.7418	35.93	12.97	0.5600	F
49	24.50	3.6304	126.95	45.84	0.5600	D,F
50	25.44	3.4984	30.80	11.12	0.5600	A,F
51	25.90	3.4373	23.68	8.55	0.5600	F
52	26.78	3.3263	1000.00	178.91	0.2775	B,F
53	27.38	3.2548	25.99	4.65	0.2775	A,F
54	27.66	3.2224	24.87	4.45	0.2775	F
55	28.32	3.1488	70.52	12.62	0.2775	F
56	28.68	3.1101	32.25	5.77	0.2775	A,F
57	29.22	3.0539	16.45	2.94	0.2775	A,F
58	29.66	3.0095	12.38	2.22	0.2775	F
59	29.84	2.9918	10.72	1.92	0.2775	F
60	30.36	2.9417	23.96	4.29	0.2775	C,F
61	30.82	2.8989	17.95	3.21	0.2775	F
62	31.16	2.8680	24.85	4.45	0.2775	D,F
63	31.38	2.8484	13.91	2.49	0.2775	F
64	31.68	2.8221	7.88	1.41	0.2775	F
65	32.08	2.7878	27.47	2.13	0.1200	F
66	32.66	2.7396	18.98	7.76	0.6339	A,F
67	33.14	2.7010	55.97	22.88	0.6339	E,F
68	33.54	2.6697	38.06	15.56	0.6339	F
69	33.70	2.6574	37.38	15.28	0.6339	D,F
70	33.94	2.6392	41.53	16.97	0.6339	A,F
71	34.34	2.6093	46.24	18.90	0.6339	A,F
72	34.52	2.5962	49.44	20.21	0.6339	A,E,F
73	34.80	2.5759	72.89	29.79	0.6339	A,F
74	35.32	2.5392	68.38	27.95	0.6339	E,F
75	35.80	2.5062	126.07	51.53	0.6339	A,C,D,E,F
76	36.08	2.4874	107.62	43.99	0.6339	A,F
77	36.74	2.4442	184.31	95.07	0.8000	A,B,E,F
78	37.00	2.4276	118.34	61.04	0.8000	A,D,F
79	39.52	2.2784	77.31	39.88	0.8000	A,B,E,F
80	40.36	2.2329	64.18	33.10	0.8000	A,B,E,F
81	41.20	2.1893	39.84	20.55	0.8000	A,D,E,F
82	42.10	2.1446	35.44	18.28	0.8000	A,D
83	42.60	2.1206	63.09	32.54	0.8000	B

84	43.68	2.0706	17.13	7.49	0.6783	A
85	44.58	2.0309	11.61	4.62	0.6174	
86	45.12	2.0078	12.71	4.56	0.5565	E
87	45.92	1.9747	37.65	7.60	0.3131	A,B
88	46.74	1.9419	7.00	1.46	0.3241	A,D
89	47.22	1.9233	10.46	2.26	0.3351	E
90	47.56	1.9103	7.96	1.05	0.2044	C
91	48.28	1.8835	14.49	0.69	0.0738	A,E
92	48.62	1.8711	5.36	0.38	0.1102	A
93	49.30	1.8469	10.62	1.00	0.1466	A
94	49.74	1.8316	6.52	0.70	0.1655	A,E
95	50.26	1.8139	125.95	22.23	0.2738	A,B,D
96	50.78	1.7965	18.92	3.34	0.2738	B,D,E
97	51.20	1.7827	16.65	2.94	0.2738	
98	51.48	1.7737	15.24	2.69	0.2738	E
99	51.94	1.7591	12.93	2.28	0.2738	
100	52.14	1.7528	12.46	2.20	0.2738	A
101	52.66	1.7367	19.58	3.46	0.2738	A,D
102	53.10	1.7233	29.60	5.23	0.2738	A
103	53.36	1.7156	42.63	7.53	0.2738	A,E
104	53.50	1.7114	42.65	7.53	0.2738	A
105	53.74	1.7043	38.35	6.77	0.2738	C
106	54.10	1.6938	34.00	6.00	0.2738	A,D,E
107	54.94	1.6699	40.22	8.76	0.3377	A,B,D,E
108	55.48	1.6549	14.51	3.16	0.3377	A,B
109	55.92	1.6429	18.04	1.40	0.1200	A
110	56.32	1.6322	20.27	1.57	0.1200	A
111	56.60	1.6248	18.26	1.41	0.1200	A
112	56.86	1.6180	7.37	0.44	0.0918	
113	57.32	1.6061	15.85	1.23	0.1200	A,B,C,E
114	57.52	1.6010	8.49	0.54	0.0979	A
115	58.22	1.5834	8.80	1.43	0.2514	A
116	58.50	1.5765	13.91	2.26	0.2514	A
117	58.72	1.5711	16.50	2.67	0.2514	A,D,E
118	59.04	1.5633	51.52	3.99	0.1200	A,E
119	59.60	1.5500	33.74	11.91	0.5473	A
120	60.04	1.5397	124.96	45.15	0.5473	A,B,D
121	60.52	1.5286	38.73	13.99	0.5473	A
122	60.86	1.5209	45.45	16.42	0.5473	A
123	61.30	1.5110	43.78	15.82	0.5473	A,E
124	61.46	1.5075	44.70	16.15	0.5473	A,D,E
125	61.78	1.5004	31.93	11.54	0.5473	A,D
126	61.98	1.4961	16.18	5.85	0.5473	A
127	62.58	1.4831	8.95	3.23	0.5473	A
128	62.84	1.4776	11.89	4.30	0.5473	A,E
129	63.02	1.4738	20.01	7.23	0.5473	A,C
130	63.28	1.4684	11.89	4.30	0.5473	A
131	63.54	1.4630	6.78	2.45	0.5473	A,D,E
132	64.08	1.4520	19.93	7.20	0.5473	A,B
133	64.28	1.4480	15.40	5.56	0.5473	A,E
134	65.80	1.4181	9.60	3.47	0.5473	A,B,D
135	66.04	1.4136	5.67	2.05	0.5473	A,C
136	67.40	1.3883	10.74	3.88	0.5473	A,C,D,E
137	67.82	1.3807	47.35	17.11	0.5473	B,E
138	68.22	1.3736	73.31	26.49	0.5473	A,B
139	68.38	1.3708	67.45	24.37	0.5473	A
140	68.92	1.3614	3.65	1.32	0.5473	A,E

Integrated Profile Areas

Based on calculated profile

Profile area	***Counts***	***Amount***
Overall diffraction profile	101526	100.00%
Background radiation	56383	55.54%
Diffraction peaks	45143	44.46%
Peak area belonging to selected phases	21134	20.82%
Peak area of phase A (Talc)	*3187*	*3.14%*
Peak area of phase B (Quartz)	*9765*	*9.62%*
Peak area of phase C (Magnetite)	*551*	*0.54%*
Peak area of phase D (Lizardite)	*2027*	*2.00%*
Peak area of phase E (Goethite)	*2617*	*2.58%*
Peak area of phase F (Antigorite)	*2987*	*2.94%*
Unidentified peak area	24009	23.65%

Peak Residuals

Peak data	***Counts***	***Amount***
Overall peak intensity	1584	100.00%
Peak intensity belonging to selected phases	1441	91.00%
Unidentified peak intensity	143	9.00%

DIFFRACTION PATTERN GRAPHICS

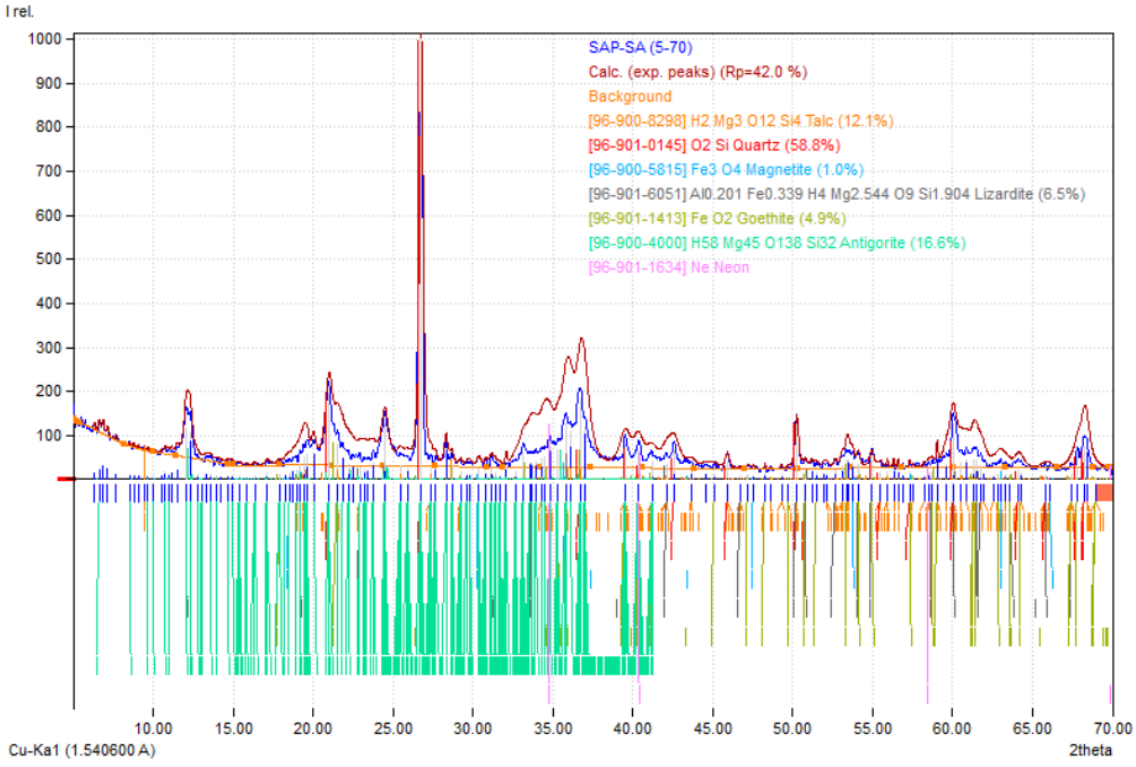

Lampiran 3 Data Analisis XRF

Analyzed Result (Multi – Land)

Analysis type : Quant analysis Analysis date : 2023- 1- 4 11:32

Analysis code : Nikel Ore 2023

No.	Sample name	Ni mass %	Co mass %	SiO_2 mass %	Al_2O_3 mass %	Fe_2O_3 mass %	CaO mass %	MgO mass %	$Li_2B_4O_7$
1	L-70	1.082	0.017	40.132	1.921	14.412	0.318	32.551	20.000
2	L-80	1.131	0.018	39.270	1.937	15.730	0.380	32.133	20.000
3	L-100	1.247	0.020	38.317	1.951	17.801	0.410	30.720	20.000
4	L-120	1.264	0.022	37.934	1.953	19.779	0.416	29.572	20.000
5	S-70	1.710	0.016	49.904	0.515	8.858	0.507	36.206	20.000
6	S-80	1.713	0.018	48.710	0.527	9.121	0.521	35.413	20.000
7	S-100	1.721	0.020	48.632	0.630	9.680	0.630	34.627	20.000
8	S-120	1.728	0.021	46.811	0.727	9.961	0.677	34.211	20.000
9	SA-Lim	1.282	0.019	38.360	1.944	17.926	0.413	31.309	20.000
10	SA-Sap	1.718	0.020	47.542	0.610	9.726	0.619	34.870	20.000
	Number	10	10	10	10	10	10	10	10
	Average	1.460	0.019	43.661	1.272	13.299	0.489	33.161	20.000
	RSD(%)	19.102	9.701	11.449	55.707	32.195	24.755	6.684	0

SUCOFINDO

Lampiran 4 Peta Pengambilan Sampel